Pergamon

Bioorganic & Medicinal Chemistry 10 (2002) 2657–2662

BIOORGANIC & MEDICINAL CHEMISTRY

Non-Thiol Farnesyltransferase Inhibitors: Utilization of an Aryl Binding Site by 5-Arylacryloylaminobenzophenones

Andreas Mitsch,[b] Markus Böhm,[b] Pia Wißner,[b] Isabel Sattler[c] and Martin Schlitzer[a,*]

[a]*Department für Pharmazie, Zentrum für Pharmaforschung, Ludwig-Maximilians-Universität München, Butenandtstraße 5-13, D-81377 München, Germany*

[b]*Institut für Pharmazeutische Chemie, Philipps-Universität Marburg, Marbacher Weg 6, D-35032 Marburg, Germany*

[c]*Hans-Knöll-Institut für Naturstoff-Forschung e.V., Beutenbergstraße 11, D-07745, Jena, Germany*

Received 30 January 2002; accepted 8 March 2002

Abstract—We recently described a novel aryl binding site of farnesyltransferase. The 2-naphthylacryloyl residue was developed as an appropriate substituent for our benzophenone-based AAX-peptidomimetic capable of occupying this binding site, resulting in a non-thiol farnesyltransferase inhibitor with nanomolar activity. The activity of this inhibitor is readily explained on the basis of docking studies which show the 2-naphthyl residue fitting into the aryl binding site. © 2002 Elsevier Science Ltd. All rights reserved.

Introduction

Over the past years, farnesyltransferase has become a major target in the development of potential anticancer drugs. Farnesyltransferase catalyzes the transfer of a farnesyl residue from farnesylpyrophosphate to the thiol of a cysteine side chain of proteins carrying the so-called CAAX-sequence at their C-terminus. C represents the cysteine to be farnesylated, A reveals amino acids normally (but not necessarily) carrying aliphatic side chains, and X mostly represents methionine or serine.[1,2]

Although farnesyltransferase inhibitors have demonstrated their efficiency in various cancer cell culture assays, animal models and first clinical studies, it turned out that their mechanism of action is much more complicated as initially supposed. Farnesyltransferase inhibitors display multiple effects, for example inhibition of anchorage independent cell growth, reversal of the phenotype of cancer cells back to that of non-transformed cells, cell cycle arrest and induction of apoptosis. It became obvious that these multiple effects cannot be attributed solely to the prevention of Ras farnesylation. Several different farnesylated proteins, as for instance Ras, RhoB and centromere binding proteins seem to be involved in the action of farnesyltransferase inhibitors. Although the exact mechanism of the antiproliferative effect remains to be determined, farnesyltransferase inhibitors are regarded as a major emerging strategy in cancer therapy.[3–12]

Most inhibitors described in literature are peptidomimetics resembling the CAAX-tetrapeptide recognition sequence of farnesylated proteins. The majority of these CAAX-peptidomimetics exhibit a free thiol group which is shown to coordinate the enzyme-bound zinc ion. However, free thiols are associated with several adverse drug effects,[13] and therefore, the development of farnesyltransferase inhibitors is clearly directed toward the so-called non-thiol farnesyltransferase inhibitors. The most frequently used replacements for cysteine are nitrogen-containing heterocycles. The ring nitrogen is supposed to coordinate to the enzyme-bound zinc similarly to the cysteine thiol group.[14] However, it has been shown that nitrogen heterocycles can be replaced by aryl residues lacking the ability to coordinate metal atoms without loosing too much of farnesyltransferase inhibitory activity.[15,16] Therefore, the existence of at least one hitherto unknown aryl binding region in the farnesyltransferase's active site has been postulated.[17,18]

Using docking studies of model compounds of non-thiol farnesyltransferase inhibitors as well as GRID analysis of farnesyltransferase's active site, we have identified two different aryl binding clefts in the active site of farnesyltransferase which we suggest to be the postulated aryl binding regions (Fig. 1a).[19]

*Corresponding author. Tel.: +49-89-2180-7804; e-mail: martin.schlitzer@cup.uni-muenchen.de

0968-0896/02/$ - see front matter
PII: S0968-0896(02)00088-3

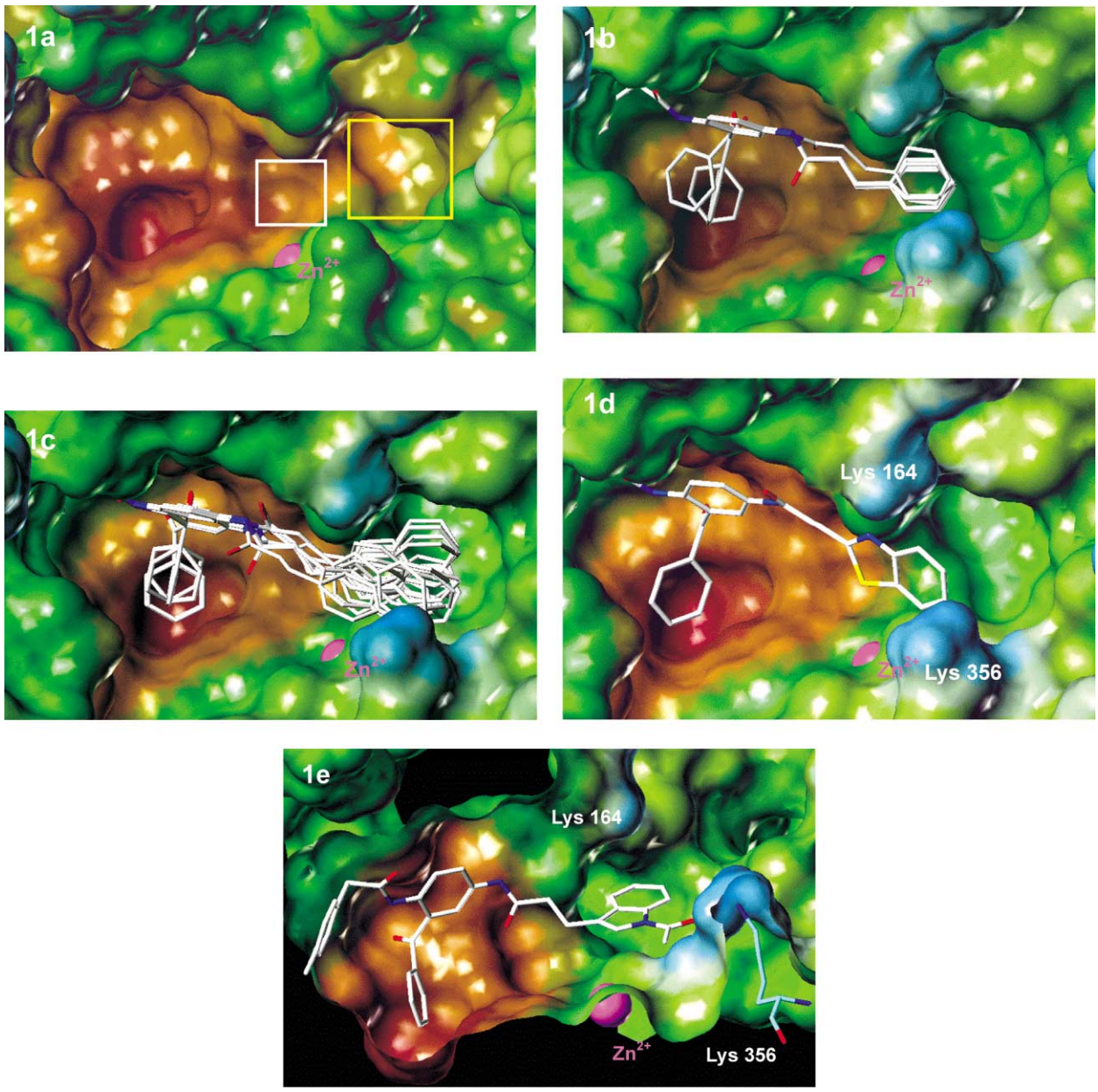

Figure 1. (a) View of the active site of farnesyltransferase. Lipophilic (brown) and hydrophilic (green to blue) properties are displayed on the Connolly surface of the enzyme. The location of the near and far aryl binding sites is indicated by a white and yellow box, respectively. (b) Representative docking solutions of the cinnamoyl-substituted inhibitor **3a**, showing that the terminal phenyl residue only partially fills the far aryl binding site. (c) Representative docking solutions of inhibitor **3b** substituted with 2-naphthylarylic acid, showing that the terminal 2-naphthyl residue occupies a larger portion of the far aryl binding site. (d) Low energy docking solution of inhibitor **3g**, showing the ring nitrogen in the vicinity of Lys 164, enabling a hydrogen bond. (e) Low energy docking solution of inhibitor **3h**, showing the 3-indolyl moiety in the aryl binding side and the carbonyl oxygen of the acetyl residue in close proximity to Lys 356, enabling a hydrogen bond. The angle of sight of this picture is different from that of the other ones.

In this study, we intended to develop an appropriate residue for our benzophenone-based AAX-peptidomimetic substructure[20] which is capable of placing an aryl moiety into the far aryl binding site.

Chemistry

Synthesis of the target compounds **3a**–**h** was accomplished by the acylation of 5-amino-2-(*p*-tolylacetylamino)benzophenone[20] (**1**) using appropriate 3-arylacrylic acid chlorides (**2**) (Scheme 1). These were prepared from the corresponding 3-arylacrylic acids which in turn were prepared by knoevenagel condensation from appropriate aldehydes and malonic acid.

Molecular modeling

The coordinates of the published structure of a ternary complex of farnesyltransferase, a farnesylpyrophosphate analogue and *N*-acetyl-Cys-Val-Ile-selenoMetOH (PDB-code 1QBQ)[21] were used for the modeling studies. The tetrapeptide was removed from the crystal structure, and the solvent accessible surface of the farnesyltransferase's active site was calculated using the program MOLCAD as implemented in the molecular modeling software

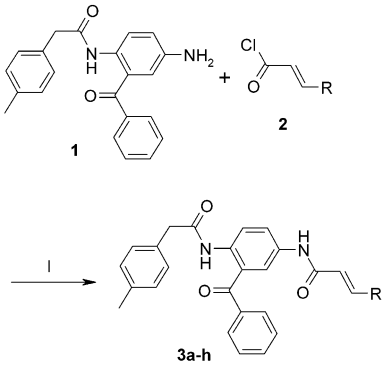

Scheme 1. (I) Toluene/dioxane, reflux, 2 h.

package SYBYL.[22] Farnesylpyrophosphate was included as part of the enzyme's molecular surface. The previously determined position of the benzophenone peptidomimetic substructure[19] was used as starting fragment for the docking of inhibitors **3a** and **3b**. Subsequently, the docking program FlexX[23] places the remaining fragments of the inhibitors in a piece-wise fashion into the active site searching for favorable hydrophobic and H-bond interactions while avoiding steric overlaps. The docking runs provided sets of solutions which were inspected according to their suggested binding energy. Obviously unreasonable solutions were excluded, for example those where major parts of the inhibitors were exposed merely to the solvent without showing specific interactions within the active site.

Farnesyltransferase inhibition assay

The inhibitory activity of the inhibitors was determined using the fluorescence enhancement assay as described by Pompliano.[24] The assay employed yeast farnesyltransferase (FTase) fused to Glutathione *S*-transferase at the N-terminus of the β-subunit.[24] Farnesylpyrophosphate and the dansylated pentapeptide Ds-GlyCysValLeuSer were used as substrates. Upon farnesylation of the cysteine thiol the dansyl residue is placed in a lipophilic environment resulting in an enhancement of fluorescence at 505 nm which is use to monitor the enzyme reaction.

Results and Discussion

Since we successfully identified the putative location of the farnesyltransferase's aryl binding sites,[19] we further set out to develop an appropriate residue for our AAX-peptidomimetic benzophenone substructure which is able to place an aryl residue into the far aryl binding site (Fig. 1a). Docking of several different possible residues suggested that cinnamic acid might be such an appropriate residue. We rationalized that the trans-configured double bond of this moiety would force the terminal aryl residue into the aryl binding cleft as shown in Figure 1b. Indeed, inhibitor **3a** carrying this cinnamoyl residue could inhibit farnesyltransferase with an IC_{50} of 2.4 μM (Table 1). The representative solutions of the docking runs (Fig. 1b), however, clearly indicate that the phenyl residue of the cinnamoyl moiety occupies

Table 1. Farnesyltransferase inhibitory activity of compounds **3a–h**

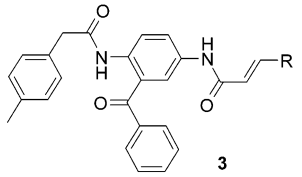

Compd	R	IC_{50} (nM)
3a		2400 ± 400
3b	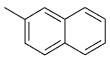	115 ± 20
3c		5600 ± 300
3d	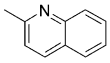	1500 ± 200
3e	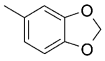	6300 ± 300
3f	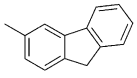	10,000 ± 500
3g	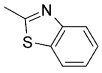	760 ± 105
3h	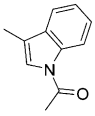	110 ± 40

only the smaller part of the far aryl binding site. Accordingly, a more bulky aryl residue connected to the 3-position of the acrylic acid substructure should fill more of the aryl binding site. Figure 1c shows representative examples of the docking runs of inhibitor **3b** substituted with 2-naphthylarylic acid. In this case, the bulky 2-naphthyl moiety is more likely to occupy the aryl binding site than the smaller phenyl residue of inhibitor **3a**. This is mirrored by a 20-fold enhancement in farnesyltransferase inhibitory activity of **3b** (IC_{50} = 115 nM) compared to inhibitor **3a**. The inhibitory activity is proved to be sensitive towards changes in geometry and electronic properties of the 3-arylacryloyl moiety. Accordingly, the 1-naphthyl analogue **3c** (IC_{50} = 5600 nM) is markedly less active than its isomer **3b**. Docking of this inhibitor (not shown) reveales that the second annellated ring does not occupy the binding cleft but is completely exposed to the solvent. Also less active are the piperonyl derivative **3e** (IC_{50} = 6300 nM) and the 2-quinonyl derivative **3d** (IC_{50} = 1500 nM). Obviously, the fluorenyl moiety of inhibitor **3f** is already too large to fit into the aryl binding site as indicated by its poor IC_{50} of 10 μM. Submicromolar activity is recorded for the 2-benzothiazolyl derivative **3g** (IC_{50} = 760 nM) and the 1-acetyl-3-indolyl derivative **3h** (IC_{50} = 110 nM), the latter one showing an inhibition rate

comparable to the 2-naphthyl substituted inhibitor **3b**. Docking of these two inhibitors provides a reasonable explanation for the compatively better activity of these compounds. Although the benzothiazole moiety of inhibitor **3g** does not fill the aryl binding site better than the phenyl residue of inhibitor **3a**, there is a possible hydrogen bond between the ring nitrogen and the side chain of Lys 164α (Fig. 1d) which may account for the 3-fold better activity of the benzothiazole derivative **3g** in comparison to the cinnamoyl derivative **3a**. No indication of an interaction of the thiazole ring of **3g** with the zinc has been found by flexible docking. Regarding the geometry of the arylacryloyl residues, compound **3h** is somewhere between the 2-naphthyl derivative **3b** and the much less active 1-nahthyl isomer **3c**. However, flexible docking reveals that the 3-indolyl moiety of **3h** nicely fitts into the aryl binding side (Fig. 1e). Furthermore, the carbonyl oxygen of the acetyl residue is placed in close proximity to the side chain of Lys 356β enabling a hydrogen bond between these two moieties.

In summary, the 2-naphthylacryloyl residue was developed as an appropriate substituent for our benzophenone-based AAX-peptidomimetic which is capable of occupying the aryl binding site of farnesyltransferase. This resulted in a non-thiol farnesyltransferase inhibitor with nanomolar activity.

Experimental

^{1}H and ^{13}C NMR spectra were recorded on a Jeol JMN-GX-400 and a Jeol JMN-LA-500 spectrometer. Mass spectra were obtained with a Vacuum Generators VG 7070H using a Vector 1 data acquisition system from Teknivent or a AutoSpec mass spectrometer from Micromass. IR spectra were recorded on a Nicolet 510P FT-IR-spectrometer. Microanalyses were obtained from a CH analyzer according to Dr. Salzer from Labormatic and from a Hewlett Packard CHN-analyzer type 185. Melting points were obtained with a Leitz microscope and are uncorrected. Column chromatography was carried out using silica gel 60 (0.062–0.200 mm) from Merck. Medium Pressure Liquid Chromatography (MPLC) was performed using a pump type 688 from Büchi and a column of 3.5 cm diameter and 45 cm length filled with silica gel 60 (0.015–0.040 mm) from Merck.

General procedure A: amide formation using acids chlorides

Arylacrylic acids were dissolved in dichloromethane and 0.2 mL oxalylchloride per mmol acid and a few drops DMF were added. The mixture was stirred at room temperature for 2 h and the volatiles were evaporated in vacuo. The residue obtained was dissolved in toluene or dioxane (approx. 10 mL) and added to a solution of one equivalent of 5-amino-2-(*p*-tolylacetylamino)benzophenone in hot toluene (approx. 50 mL). The mixture was heated under reflux for 2 h. Then, the solvent was removed in vacuo to give the crude products.

***N*-3-Benzoyl-4-(p-tolylacetylamino)phenyl-3-phenylacrylamide (3a).** From cinnamic acid (148 mg, 1 mmol) according to general procedure A. Purification: recrystallization from toluene. Yield 214 mg (45%); mp 97 °C. IR (KBr): ν = 3440, 3264, 3086, 1668, 1631, 1547, 1504 cm^{-1}. ^{1}H NMR ($CDCl_3$): δ 2.31 (s, 3H), 3.67 (s, 2H), 6.45 (d, J = 16 Hz, 1H), 7.15 (m, 3H), 7.24 (m, 3H), 7.34 (m, 3H), 7.45 (m, 4H), 7.54–7.60 (m, 2H), 7.69 (m, 2H), 8.01 (s, 1H), 8.51 (m, 1H), 10.52 (s, 1H). MS (EI): m/z 474 (100) M^+, 342 (39), 212 (37), 131 (34). Anal. calcd for $C_{31}H_{26}N_2O_3$: C, 78.46; H, 5.52; N, 5.90; found: C, 78.71; H, 5.52; N, 5.86.

***N*-3-Benzoyl-4-(*p*-tolylacetylamino)phenyl-3-naphthalen-2-yl-acrylamide (3b).** From 3-naphtalen-2-yl-acrylic acid (297 mg, 1.5 mmol) according to general procedure A. Purification: recrystallization from toluene. Yield 465 mg (88%); mp 97C. IR (KBr): ν = 3418, 3056, 1674, 1634, 1554, 1508 cm^{-1}. ^{1}H NMR ($CDCl_3$): δ 2.24 (s, 3H), 3.60 (s, 2H), 6.48 (d, J = 16 Hz, 1H), 7.09 (m, 2H), 7.17 (m, 3H), 7.36–7.43 (m, 4H), 7.49 (m, 3H), 7.63 (m, 2H), 7.68–7.77 (m, 5H), 7.98 (s, 1H), 8.44 (m, 1H), 10.46 (s, 1H). MS (EI): m/z 181 (100), 212 (18), 105 (73), 154 (43), 344 (37), 524 (28) M^+. Anal. calcd for $C_{35}H_{28}N_2O_3$: C, 80.13; H, 5.38; N, 5.34; found: C, 79.80; H, 5.40; N, 5.28.

***N*-3-Benzoyl-4-(*p*-tolyl-acetylamino)phenyl-3-naphthalen-1-yl-acrylamide (3c).** From 3-naphtalen-1-yl-acrylic acid (298 mg, 1.5 mmol) according to general procedure A. Purification: recrystallization from toluene. Yield 522 mg (66%); mp 134 °C. IR (KBr): ν = 3292, 3055, 2921, 1655, 1596, 1542, 1507 cm^{-1}. ^{1}H NMR ($CDCl_3$): δ 2.25 (s, 3H), 3.61 (s, 2H), 6.47 (d, J = 16 Hz, 1H), 7.08 (m, 2H), 7.18 (m, 3H), 7.34–7.65 (m, 10H), 7.79 (m, 2H), 8.00 (s, 1H), 8.08 (m, 1H), 8.45 (m, 2H), 10.46 (s, 1H). MS (EI): m/z 181 (100), 105 (51), 212 (43), 524 (33) M^+. Anal. calcd for $C_{35}H_{28}N_2O_3$: C, 80.13; H, 5.38; N, 5.34; found: C, 79.84; H, 5.43; N, 5.35.

***N*-3-Benzoyl-4-(*p*-tolylacetylamino)phenyl-3-quinolin-2-yl-acrylamide (3d).** From 3-quinolin-2-yl-acrylic acid (199 mg, 1 mmol) according to general procedure A. Purification: recrystallization from toluene. Yield 220 mg (42%); mp 187 °C. IR (KBr): ν = 3438, 1641, 1556, 1507 cm^{-1}. ^{1}H NMR ($CDCl_3$): δ 2.26 (s, 3H), 3.63 (s, 2H), 7.10 (m, 2H), 7.19 (m, 4H), 7.39–7.54 (m, 5H), 7.61–7.65 (m, 3H), 7.71 (m, 1H), 7.75 (d, J = 16 Hz, 1H), 7.86 (s, 1H), 7.95 (m, 2H), 8.07 (m, 1H), 8.46 (m, 1H), 10.46 (s, 1H). MS (EI): m/z 182 (100), 105 (42), 212 (36), 525 (34) M^+, 420 (34). Anal. calcd for $C_{34}H_{27}N_3O_3$: C, 77.70; H, 5.18; N, 7.99; found: C, 77.32; H, 5.29; N, 7.71.

3-Benzo[1,3]dioxol-5-yl-*N*-3-benzoyl-4-(2-*p*-tolylacetylamino)phenylacrylamide (3e). From piperonyl-acrylic acid (192 mg, 1.5 mmol) according to general procedure A. Purification: column chromatography (EtOAc/hexane 3:2) and subsequent recrystallization from toluene. Yield 106 mg (14%); mp 185°C. IR (KBr): ν = 3332, 3043, 2907, 1672, 1551, 1506 cm^{-1}. ^{1}H NMR ($CDCl_3$): δ 2.26 (s, 3H), 3.62 (s, 2H), 5.92 (s, 2H), 6.21 (d, J = 16 Hz, 1H), 6.72 (m, 1H), 6.89 (m, 2H), 7.09 (m, 2H), 7.18 (m, 2H), 7.32 (m, 1H), 7.41 (m, 2H), 7.51 (m, 3H), 7.64 (m, 2H), 7.93 (s, 1H), 8.47 (m, 1H), 10.47 (s, 1H). MS (EI): m/z 175 (100), 145 (51), 212 (50),105 (38), 518 (23) M^+.

Anal. calcd for $C_{32}H_{26}N_2O_5$: C, 74.12; H, 5.05; N, 5.40; found: C, 73.99; H, 5.06; N, 5.46.

***N*-3-Benzoyl-4-(*p*-tolylacetylamino)phenyl-3-(9H-fluoren-2-yl)-acrylamide (3f).** From 3-(fluoren-2-yl)acrylic acid (236 mg, 1 mmol) according to general procedure A. Purification: MPLC (EtOAc/hexane 1:1). Yield 330 mg (59%); mp 210 °C. IR (KBr): ν = 3317, 3046, 1682, 1669, 1648, 1616, 1560, 1510 cm^{-1}. ^1H NMR ($CDCl_3$): δ 2.30 (s, 3H), 3.67 (s, 2H), 3.81 (s, 2H), 6.49 (d, $J = 16$ Hz, 1H), 7.14 (m, 2H), 7.22 (m, 2H), 7.28–7.37 (m, 2H), 7.43 (m, 3H), 7.49–7.55 (m, 4H), 7.68 (m, 4H), 7.74 (m, 1H), 7.98 (s, 1H), 8.07 (s, 1H), 8.49 (m, 1H), 10.54 (s, 1H). MS (EI): *m*/*z* 219 (100), 43 (87), 41 (36), 73 (35), 562 (19) M^+. Anal. calcd for $C_{38}H_{30}N_2O_3$: C, 81.11; H, 5.37; N, 4.98; found: C, 80.85; H, 5.50; N, 5.14.

3-Benzothiazol-2-yl-*N*-3-benzoyl-4-(*p*-tolylacetylamino)-phenylacrylamide (3g). From 3-benzothiazol-2-yl-acrylic acid (92 mg, 0.45 mmol) according to general procedure A. Purification: recrystallization from ethanol. Yield 14 mg (6%); mp 232 °C. IR (KBr): ν = 3431, 1654, 1558, 1508 cm^{-1}. ^1H NMR (DMSO-d_6): δ 2.23 (s, 3H), 3.36 (s, 2H), 6.95 (m, 1H), 6.99 (m, 2H), 7.04 (m, 2H), 7.20 (d, $J = 16$ Hz, 1H), 7.49 (m, 3H), 7.55 (m, 1H), 7.62 (m, 2H), 7.68 (m, 2H), 7.78 (m, 1H), 7.88 (m, 1H), 8.04 (m, 1H), 8.13 (m, 1H), 10.04 (s, 1H), 10.56 (s, 1H). MS (EI): *m*/*z* 105 (100), 188 (90), 212 (74), 40 (62), 531 (22) M^+. Anal. calcd for $C_{32}H_{25}N_3O_5S$: C, 72.30; H, 4.74; N, 7.90; found: C, 71.91; H, 4.34; N, 8.28.

3-(1-Acetyl-1H-indol-3-yl)-*N*-3-benzoyl-4-(*p*-tolylacetyl-amino)phenylacrylamide (3h). From 3-(1-acetyl-3-indolyl) acrylic acid (229 mg, 1 mmol) according to general procedure A. Purification: MPLC (EtOAc/hexane 1:1). Yield 333 mg (60%); mp 199 °C. IR (KBr): ν = 3273, 3136, 3083, 1664, 1623, 1544, 1505 cm^{-1}. ^1H NMR ($CDCl_3$): δ 2.26 (s, 3H), 2.55 (s, 3H), 3.66 (s, 2H), 6.65 (d, $J = 16$ Hz, 1H), 7.05 (m, 2H), 7.21 (m, 3H), 7.33 (m, 1H), 7.40 (m, 2H), 7.49–7.55 (m, 3H), 7.69 (m, 2H), 7.73 (m, 2H), 8.04 (s, 1H), 8.29 (s, 1H), 8.42 (m, 2H), 10.48 (s, 1H). MS (EI): *m*/*z* 212 (100), 170 (69), 344 (61), 555 (37) M^+. Anal. calcd for $C_{35}H_{29}N_3O_4$: C, 75.65; H, 5.26; N, 7.56; found: C, 75.51; H, 5.46; N, 7.56.

Molecular modeling

Molecular modeling was carried out using SYBYL[22] version 6.6/6.7 running on a Silicon Graphics O2 (R10000). Flexible docking was performed using FlexX[23] version 1.7.6. The FlexX command MAPREF and the perturbate mode of the PLACEBAS command were used. Default parameters were employed except the MAX_ENERGY value which was set to 10 kJ mol^{-1}.

Enzyme preparation

Yeast farnesyltransferase was used as a fusion protein to Glutathione *S*-transferase at the N-terminus of the β-subunit. Farnesyltransferase was expressed in *Escherichia coli* DH5α grown in LB media containing ampicillin and chloramphenicol for co-expression of pGEX-DPR1 and pBC-RAM2 for farnesyltransferase production.[25] The enzyme was purified by standard procedures with glutathione-agarose beads for selective binding of the target protein.

Farnesyltransferase assay

The assay was conducted as described.[24] Farnesylpyrophosphate (FPP) was obtained as a solution of the ammonium salt in methanol/10 mM aqueous NH_4Cl (7:3) from Sigma-Aldrich. Dansyl-GlyCysValLeuSer (Ds-GCVLS) was custom synthesized by ZMBH, Heidelberg, Germany. The assay mixture (100 L volume) contained 50 mM Tris/HCl pH 7.4, 5 mM $MgCl_2$, 10 M $ZnCl_2$, 5 mM dithiothreitol (DTT), 7 M Ds-GCVLS, 20 M FPP and 5 nmol (approx.) yeast GST-farnesyltransferase and 1% of various concentrations of the test compounds dissolved in dimethylsulfoxide (DMSO). The progress of the enzyme reaction was followed by monitoring the enhancement of the fluorescence emission at 505 nm (excitation 340 nm). The reaction was started by addition of the enzyme and run in a Quartz cuvette thermostatted at 30 °C. Fluorescence emission was recorded with a Perkin-Elmer LS50B spectrometer. IC_{50} values (concentrations resulting in 50% inhibition) were calculated from initial velocity of three independent measurements of four to five different concentrations of the respective inhibitor.

Acknowledgements

The authors thank Prof. Dr. G. Klebe who provided us with all facilities needed for the modeling and Ms. K. Burk for technical assistance. The pGEX-DPR1 and pBC-RAM2 plasmids were kindly provided by Prof. F. Tamanoi (UCLA). Financial support by the Deutsche Pharmazeutische Gesellschaft is gratefully acknowledged. I.S. wishes to thank Prof. Dr. S. Grabley for generous support and Ms. S. Egner for technical assistance.

References and Notes

1. Zhang, F. L.; Casey, P. J. *Annu. Rev. Biochem.* **1996**, *65*, 241.
2. Fu, H.-W.; Casey, P. J. *Rec. Prog. Hormon Res.* **1999**, *54*, 315.
3. Leonard, D. M. *J. Med. Chem.* **1997**, *40*, 2971.
4. Qian, Y. S.; Sebti, M.; Hamilton, A. D. *Biopolymers* **1997**, *43*, 25.
5. Williams, T. M. *Exp. Opin. Ther. Pat.* **1998**, *8*, 553.
6. Williams, T. M. *Exp. Opin. Ther. Pat.* **1999**, *9*, 1263.
7. Williams, T. M.; Dinsmore, C. J. *Adv. Med. Chem.* **1999**, *4*, 273.
8. Wittinghofer, A.; Waldmann, H. *Angew. Chem.* **2000**, *112*, 4360. Wittinghofer, A.; Waldmann, H. *Angew. Chem. Int. Ed.* **2000**, *39*, 4192.
9. Rowinsky, E. K.; Patnaik, A. *Emerg. Drugs* **2000**, *5*, 161.
10. Sebti, S. M.; Hamilton, A. D. *Oncogene* **2000**, *19*, 6584.
11. Cox, A. D. *Drugs* **2001**, *61*, 723.
12. Bell, I. M. *Exp. Opin. Ther. Pat.* **2000**, *10*, 1813.
13. Reynolds, J. E. F. Ed. *Martindale The Extra Pharmacopeia*, 31st ed.; Royal Pharmaceutical Society of Great Britain: London, 1996; p 821.
14. Hunt, J. T.; Lee, V. G.; Leftheris, K.; Seizinger, B.; Carboni, J.; Mabus, J.; Ricca, C.; Yan, N.; Manne, V. *J. Med. Chem.* **1996**, *39*, 353.

15. O'Connor, S. J.; Barr, K. J.; Wang, L.; Sorensen, B. K.; Tasker, A. S.; Sham, H.; Ng, A.-C.; Cohen, J.; Devine, E.; Cherian, S.; Saeed, B.; Zhang, H.; Lee, J. Y.; Warner, R.; Tahir, S.; Kovar, P.; Ewing, P.; Alder, J.; Mitten, M.; Leal, J.; Marsh, K.; Bauch, J.; Hoffman, D. J.; Sebti, S. M.; Rosenberg, S. H. *J. Med. Chem.* **1999**, *42*, 3701.
16. Augeri, D. J.; Janowick, D.; Kalvin, D.; Sullivan, G.; Larsen, J.; Dickman, D.; Ding, H.; Cohen, J.; Lee, J.; Warner, R.; Kovar, P.; Cherian, S.; Saeed, B.; Zhang, H.; Tahir, S.; Ng, S.-C.; Sham, H.; Rosenberg, S. H. *Bioorg. Med. Chem. Lett*. **1999**, *9*, 1069.
17. Breslin, M. J.; deSolms, J.; Giuliani, E. A.; Stokker, G. E.; Graham, S. L.; Pompliano, D. L.; Mosser, S. D.; Hamilton, K. A.; Hutchinson, J. H. *Bioorg. Med. Chem. Lett*. **1998**, *8*, 3311.
18. Ciccarone, T. M.; MacTough, S. C.; Williams, T. M.; Dinsmore, C. J.; O'Neill, T. J.; Shah, D.; Culberson, J. C.; Koblan, K. S.; Kohl, N. E.; Gibbs, J. B.; Oliff, A. I.; Graham, S. L.; Hartman, G. D. *Bioorg. Med. Chem. Lett*. **1999**, *9*, 1991.
19. Böhm, M.; Mitsch, A.; Wißner, P.; Sattler, I.; Schlitzer, M. *J. Med. Chem*. **2001**, *44*, 3117.
20. Sakowski, J.; Böhm, M.; Sattler, I.; Dahse, H.-M.; Schlitzer, M. *J. Med. Chem*. **2001**, *44*, 2886.
21. Strickland, C. L.; Windsor, W. T.; Syto, R.; Wang, L.; Bond, R.; Wu, R.; Schwartz, J.; Le, H. V.; Beese, L. S.; Weber, P. C. *Biochemistry* **1998**, *37*, 16601.
22. *SYBYL Molecular Modeling Software*; Tripos Inc.: 1699 South Hanley Rd, Suite 303, St. Louis, MO 63144, USA.
23. Klebe, G.; Mietzner, T.; Weber, F. *J. Comput. Aided Mol. Des* **1994**, *8*, 751.
24. Pompliano, D. L.; Gomez, R. P.; Anthony, N. J. *J. Am. Chem. Soc*. **1992**, *114*, 7945.
25. Del Villar, K.; Mitsuzawa, H.; Yang, W.; Sattler, I.; Tamanoi, F. *J. Biol. Chem*. **1997**, *272*, 680.